Ultra-low Loss CMOS Compatible Multi-Layer Si_3N_4-on-SOI Platform for 1310nm Wavelength

Ying Huang[1], Xiaoguang Tu[2], Andy Eu-Jin Lim, Junfeng Song, Tsung-Yang Liow and Guo-Qiang Lo
*Institute of Microelectronics, A*STAR (Agency for Science, Technology and Research), 11 Science Park Road, Science Park II, Singapore*
[1]huangy@ime.a-star.edu.sg; [2]tux@ime.a-star.edu.sg

Abstract: We demonstrated the applications of our Si_3N_4-on-SOI platform for O-band operation with propagation and interlayer transition loss of ~0.24dB/cm and ~0.2dB, respectively. We also characterized our SOI-based Ge photo-detector and silicon modulator at λ= 1310nm.
OCIS codes: (130.3120) Integrated Optics Devices; (230.7370) Waveguides; (250.5300) Photonic Integrated Circuits

1. Introduction

Multi-layer platform has emerged in the recent years to advance silicon photonics technology from the conventional silicon-on-insulator (SOI) platform [1-4]. Leveraging on the material diversity and vertical integration capability, the platform offers various revenues in pushing for denser integration [1], lower loss [2], better fabrication tolerance [3] and device performance [4], to propel silicon photonics technology into advance applications such as Quantum key distribution [5] and dense port count data-center optical interconnect [6]. These applications however often require O-band operation, which is incompatible with the existing platforms demonstrated in the 1550nm wavelength. Recently, we have developed a backend integrated Si_3N_4-on-SOI platform based on sequential optical layer deposition [7]. The platform uses SOI as the bottom optical layers, enabling seamless integration with the existing established SOI active devices technology [8]. High-performance devices based on dual layer design have also been demonstrated [9]. In this work, we report our recent effort to extend the platform into 1310nm wavelength windows. Both inter- and intra-optical layer losses are investigated. Active devices on the SOI platform are also characterized. Their performances are comprehensively benchmarked against similar devices in the 1550nm wavelength.

2. Multi-layer platform loss characterization

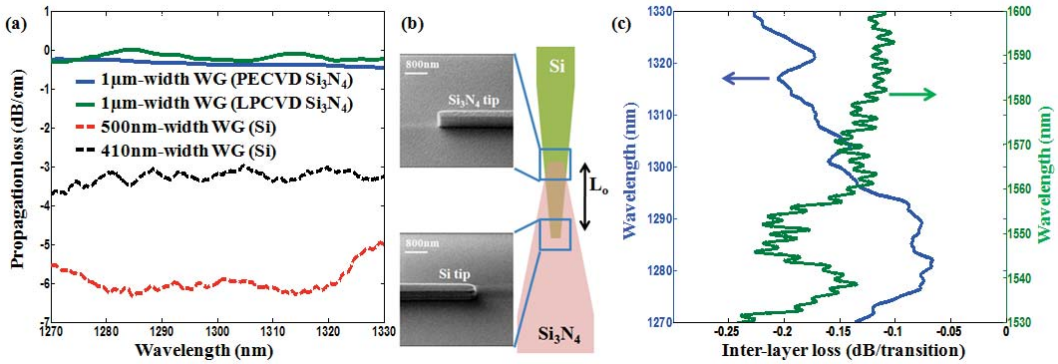

Fig. 1. (a) Propagation loss for various waveguide material, (b) Schematic diagram and SEM images of the inter-layer transition coupler, (c) Inter-layer transition loss for both 1310nm and 1550nm wavelengths.

A detailed description of our integration flow can be found in [7]. Besides the bottom SOI layer, top optical layers are constructed using plasma-enhanced chemical vapor deposition (PECVD) Si_3N_4, enabling fabrication simplicity and low loss for vertical scalability. In this section, we characterize the intra- and inter-optical layer losses in the platform, which is the other essential factor to determine the scalability of platform. Figure 1(a) illustrates the propagation loss for the different optical layers. The propagation loss of the PECVD Si_3N_4 waveguide is less than 0.5dB/cm across the measured wavelength in the O-band, which is limited by our measurement set-up. 0.24dB/cm propagation loss is observed at λ=1270nm. This is comparable with the loss performance obtained from the low pressure CVD (LPCVD) counterpart, due to the absence of absorptive N-H bond. On the other hand, 500nm-width Si waveguide, which is conventionally used for the 1550nm wavelength, shows ~ 6dB/cm losses. 410nm-width provides a much better choice for bus waveguide in the 1310nm wavelength, with a propagation loss of ~3.3dB/cm. The difference could be due to the mode-beating in the bend region for the wider waveguides.

Figure 1(b) shows the design of our transition coupler to facilitate low inter-layer coupling loss, together with the scanning electron microscopy (SEM) images of the fabricated tip. Waveguides in both layers are adiabatically tapered towards each other, with a tip width of 200nm and 300nm on the Si and Si_3N_4 layers, respectively. The taper length is 50μm for both layers. Figure 1(c) plots the transition loss for the optimized transition coupler, for both 1310nm and 1550nm wavelength windows. The overlap length (L_o) is 50 μm. The losses are extracted by linearly fitting the insertion loss curve from six devices with different number of TC inserted in it. The measured loss is ~ 0.2dB/transition for both wavelength windows, which is the lowest among all the multi-layer platforms [2, 3]. Table 1 compares the platform losses in various reported platform for different wavelengths.

Table 1. Performance benchmarking of multi-layer platforms losses at different wavelengths

Wavelengths	Intra-layer propagation loss				Inter-layer loss (per transition)			
	PECVD Si_3N_4 WG		LPCVD Si_3N_4 WG	Si WG				
	[1]	This work	This work	This work	[2]	[3]	[4]	This work
1580nm	1dB/cm	0.8dB/cm	0.4dB/cm	2.5dB/cm	>0.4dB	N.A.	N.A.	0.12dB
1550nm	3.1dB/cm	3.5dB/cm	1.3dB/cm	2.85dB/cm	N.A.	0.5dB	<0.37dB.	0.21dB
1270nm	N.A.	0.24dB/cm	0.32dB/cm	3.6dB/cm	N.A.	N.A.	N.A.	0.14dB

3. Active SOI devices characterization

To fully advance into the actual applications, the platform needs to be supported by a comprehensive device library operating in the 1310nm wavelength. In this section, we characterize our baseline active devices in the O-band, particularly the photo-detector and modulator [8]. Although the reported devices are fabricated on the SOI platform, their results can be readily extended to the multi-layer platform. This is due to the use of low temperature (400°C) PECVD Si_3N_4 in our platform, facilitating seamless integration of active devices without performance degradation [7]. Figure 2(a) shows the SEM images of the photo-detector after Germanium (Ge) growth. The device has a width and length of 8μm and 25μm, respectively. Figure 2(b) illustrates the I-V curve of the photo-detector under different bias voltage. The dark current is 590nA @ -1V bias voltage. By normalizing out the fiber coupling and waveguide propagation loss, we obtained a responsivity of ~ 0.5A/W @ -1V bias voltage. This is smaller than the 0.7A/W value measured at λ=1550nm, due to the linear scaling of internal responsivity with respect to the wavelength. The normalized S21 frequency response of the photo-detector in the 1310nm wavelength (blue line) is shown in Fig. 2(c), together with data in the 1550nm wavelength (green line). The bias voltage is -2V. The 3dB bandwidth is measured at 18.1GHz and 16.6GHz for 1310nm and 1550nm wavelengths, respectively.

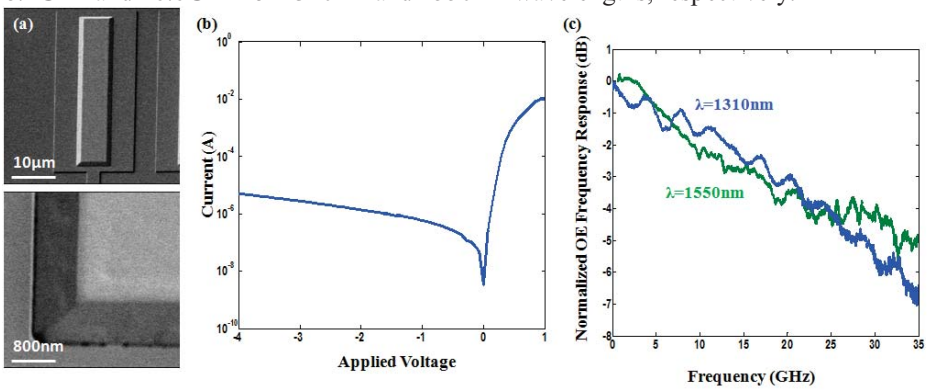

Fig. 2. (a) SEM images, (b) IV curve, (c) Normalized S21 frequency response of the photo-detector for both 1310nm and 1550nm wavelengths.

Next, we characterize the silicon optical modulator performance, using our recently reported shield coplanar waveguide (CPW) electrodes [10]. Figure 3(a) illustrates the output spectra for different bias voltages. For 5.5mm-long phase shifter, the V_π are measured at 3.0V and 4.0V for the 1310nm (blue curves) and 1550nm (green curves), respectively. The lower V_π in the shorter wavelength could be due to the stronger optical confinement. Modulation efficiency ($V_\pi \cdot L_\pi$) increases rapidly at low bias voltages and gradually saturates toward larger bias, as shown in Fig. 3(b). Better modulation efficiency is observed at λ=1310nm across all bias voltages. On the other hand, phase-shifter loss is higher for the shorter wavelength, with a quasi-linear trend. The normalized frequency response of the CPW modulator without shield at -5V bias voltage is displayed in Fig. 3(c). The 3dB bandwidth is measured at 22GHz and 17.7GHz for 1310nm and 1550nm wavelength, respectively. A large signal testing is also performed.

Under V_{bias}=-5.0V and V_{pp}=1.3V, we obtained an extinction ratio of 5.66dB and 5.97dB at λ=1310nm and λ=1550nm, respectively. The photo-detector and modulator performance for the two wavelengths are summarized in Table 2. In general, active devices show comparable or better performance in the 1310nm wavelength.

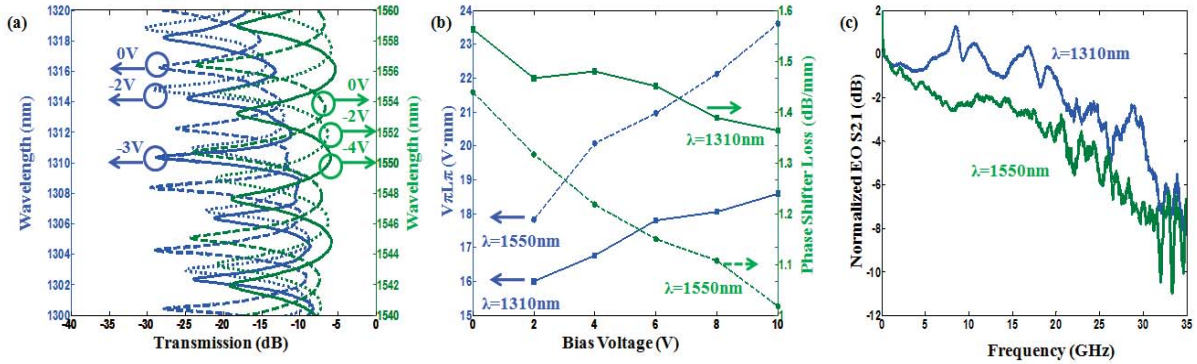

Fig. 3. (a) Output spectra of the silicon modulator with shield-CPW electrode; (b) change of $V_\pi \cdot L_\pi$ and phase shifter loss with respect to bias voltage and (c) normalized EO S21 frequency response for both 1310nm and 1550nm wavelengths.

Table 2. Performance comparison for photo-detector and modulator in different wavelengths

Wavelength	Photo-detector		Modulator			
	3dB bandwidth	Responsivity	V_π	Phase shifter loss	3dB bandwidth	E.R. @ 28Gb/s
1310nm	18.1GHz	~0.5A/W	3.0V	-1.39dB/mm	22GHz V_{bias} =-5V	5.66dB
1550nm	16.6GHz	~0.7A/W	4.0V	-0.94dB/mm	17.7 GHz V_{bias} =-5V	5.97dB

4. Conclusion

In summary, we presented our recent effort on the Si_3N_4-on-SOI platform for 1310nm wavelength operation. Ultra-low intra- (~0.24dB/cm) and inter- (~0.2dB/transition) optical layers losses are achieved, ensuring superior link budget for ultimate scalability. This is the lowest loss among all reported monolithic multi-layer platform. We also characterized our SOI-platform active devices for O-band operation. The photo-detector and modulator show comparable or better performance in these wavelengths, as compared to the traditional 1550nm telecom windows. In particular, silicon optical modulators display better modulation efficiency and 3dB-bandwidth in these wavelengths. These results validate the feasibility and capability of our Si_3N_4-on-SOI multi-layer platform to further advance silicon photonics technology from the current SOI platform, into advance applications required O-band operation.

This work was supported by the Science and Engineering Research Council of A*STAR (Agency for Science, Technology and Research), Singapore. The SERC grant number is 1323300001.

5. References

[1] N. S. Droz, and M. Lipson, "Scalable 3D dense integration of photonic on bulk silicon," Opt. Express **19**, 17758-17765 (2011).
[2] J. F. Bauters, M. L. Davenport, M. Heck, J. Doylend, A. Chen, A. Fang and J. Bowers, "Silicon on ultra-low-loss waveguide photonic integration platform," Opt. Express **21**, 544-555 (2013).
[3] L. Chen, C. Doerr, L. Buhl, Y. Baeyens and R. Aroca, "Monolithically integrated 40-wavelength demultiplexer and photodetector array on silicon," IEEE Photonics Technol. Lett. **23**, 869-871 (2011).
[4] T. Tsuchizawa, K. Yamada, T. Watanabe, S. Park, H. Nishi, R. Kou, H. Shinojima and S. Itabashi, "Monolithic integration of silicon-, germanium-, and silica-based optical devices for telecommunications applications," IEEE J. Sel. Topics in Quant. Elec. **17**, 516-525 (2011).
[5] M. T. Liu, Y. Huang, W. Wang, and H. C. Lim, "Broadband quantum-correlated photon-pairs in the O-band generated from a dispersion-engineered silicon waveguide," in Conference on Lasers and Electro-Optics Europe/International Quantum Electronics Conference (CLEO Europe/IQEC), Munich, Germany, 2013, IB-P.19.
[6] H. Guan, A. Novack, M. Streshinsky, R. Shi, Y. Liu, Q. Fang, A. Lim, G. Q. Lo, T. Baehr-Jones and M. Hochberg, "high efficiency low-crosstalk 1310-nm polarization splitter and rotator," IEEE Photonics Technol. Lett. **26**, 925-928 (2014).
[7] Y. Huang, J. Song, X. Luo, T.Y. Liow, and G.Q. Lo, "CMOS compatible monolithic multi-layer Si3N4-on-SOI platform for low-loss high performance silicon photonics dense integration," Opt. Express **22**, 21859-21865 (2014).
[8] T. Y. Liow, K. Ang, Q. Fang, J. Song, Y. Xiong, M. Yu, G. Q. Lo and D. Kwong, "Silicon modulators and Germanium photodetectors on SOI: monolithic integration, compatibility, and performance optimization," IEEE J. Sel. Topics in Quant. Elec. **16**, 307-315 (2010).
[9] Wesley D. S., Y. Huang, D. Liang, T. Barwicz, B. J. F. Taylor, G.Q. Lo, and Joyce K. S. Poon, "Wide bandwidth and high coupling efficiency Si3N4-on-SOI dual-level grating coupler ", Opt. Express **22**, 10938-10947 (2014).
[10] X. Tu, K. Chang, T. Y. Liow, J. Song , X. Luo, L. Jia, Q. Fang, M. Yu, G. Q. Lo, P. Dong and Y. K. Chen, "Silicon optical modulator with shield coplanar waveguide electrodes," Opt. Express **22**, 23724-23731 (2014).